Ecosystems
https://doi.org/10.1007/s10021-023-00872-y

ECOSYSTEMS

Current Forest–Savanna Transition in Northern South America Departs from Typical Climatic Thresholds

Santiago Valencia,[1,2]* Juan F. Salazar,[1] Natalia Hoyos,[3] Dolors Armenteras,[4] and Juan Camilo Villegas[2]

[1]Grupo GIGA, Escuela Ambiental, Facultad de Ingeniería, Universidad de Antioquía, Medellín, Colombia; [2]Grupo de Investigación en Ecología Aplicada, Escuela Ambiental, Facultad de Ingeniería, Universidad de Antioquía, Medellín, Colombia; [3]Department of History and Social Sciences, Universidad del Norte, Barranquilla, Colombia; [4]Grupo de Ecología del Paisaje y Modelación de Ecosistemas ECOLMOD, Departamento de Biología, Facultad de Ciencias, Universidad Nacional de Colombia, Bogotá, Colombia

Abstract

The forest–savanna transition is the most widespread ecotone in the tropics, with important ecological, climatic, and biogeochemical implications at local to global scales. However, the factors and mechanisms that control this transition vary among continents and regions. Here, we analyzed which factors best explain the transition in northern South America (Llanos ecoregion and northwestern Amazon), where common thresholds on typical environmental factors (for example, mean annual precipitation (MAP), wet season precipitation) fail to predict it. For instance, savannas in the Llanos occur at MAP levels (> 1500 mm) which are typical of forests in other tropical regions. We examined the transition's climate features, soils, and disturbance (fire frequency) spaces using remotely sensed data. We used logistic generalized linear models to assess the effect of seasonal (season length) and intra-seasonal (daily precipitation frequency and intensity) precipitation metrics during the dry season, soil silt content, and fire frequency, on the transition using canopy cover, tree cover, and the maximum Plant Area Volume Density as vegetation structure descriptor variables. Fire frequency and precipitation frequency were the most important variables explaining the transition. Although most fires occur in savannas, we found that a significant percentage of savanna pixels (46%) had no fires. This study indicates that the transition should be characterized regionally in response to biogeographic differences (for example, climatic space) among regions and continents. Our results highlight the importance of fire frequency and intra-seasonal precipitation in determining the transition in northern South America. Furthermore, future studies should consider regional differences in the climatic space of forest and savanna to improve projections of global change impacts on these highly diverse ecosystems.

Key words: climatic space; fire frequency; forest; savanna transition; humid tropical forest; llanos ecoregion; intra-seasonal precipitation.

Received 8 September 2022; accepted 23 July 2023

Supplementary Information: The online version contains supplementary material available at https://doi.org/10.1007/s10021-023-00872-y.

Author Contributions SV, JFS, and JCV conceived and designed the study, analyzed the data, and wrote the first draft of the manuscript. SV performed the research. NH and DA completed the manuscript and made important contributions to interpreting the results and to writing the final version of manuscript.

*Corresponding author; e-mail: santiago.valencia8@udea.edu.co

Published online: 25 August 2023

Highlights

- Forest–savanna transition drivers vary globally, but not yet explored in northern South America.
- In the Llanos, Savannas occur in forest expected climate space.
- Fire and dry season precipitation frequency best explains the transition.

Introduction

Tropical forests and savannas account for more than 60% of the terrestrial productivity (Beer and others 2010). Both ecosystems are globally strategic, as their presence and dynamics have important ecological, climatic, and biogeochemical implications (Oliveras and Malhi 2016). In the tropics, this is the most widespread and, perhaps, the most dynamic ecotone. However, the processes and mechanisms that control this transition vary among regions and remain not fully understood (Lehmann and others 2014; Archibald and others 2019). More specifically, this transition is influenced by multiple interactions between vegetation and environmental factors such as climate, soil properties, fire, and herbivory, which operate at different spatiotemporal scales (Oliveras and Malhi 2016).

In tropical regions, water availability—which results from the interaction between vegetation, climate, and soil properties—has been identified as one of the major determinants of ecosystem structure and distribution (Oliveras and Malhi 2016; Gosling and others 2022). For instance, both in situ and remotely sensed observations show that tropical forests occur more often in regions with higher mean annual precipitation (MAP) and shorter dry seasons than savannas (Lehmann and others 2011; Archibald and others 2019; Jaramillo 2023). However, there is not a simple precipitation threshold that defines the distribution or transition between forests and savannas (Archibald and others 2019; Ciemer and others 2019; Staal and others 2020). For example, both savanna and forest occur in regions with intermediate MAP values (between 1000 and 2500 mm globally; Staver and others 2011). In those regions, other factors such as the interactions between climate, vegetation, soil, and disturbance regimes (for example, fire and herbivory) appear to explain the transition between these ecosystems (Oliveras and Malhi 2016). Several studies highlight how, in addition to MAP, seasonal (for example, length and magnitude of wet and dry seasons) and intra-seasonal precipitation (for example, frequency and intensity of daily precipitation) metrics can improve the description and prediction of tropical forest and savanna distribution (for example, Xu and others 2018; Hoyos and others 2022) via its effects on water availability. This highlights the importance of understanding the effect of seasonal and intra-annual precipitation metrics on ecosystem distribution, particularly when climate models predict changes in precipitation properties (such as precipitation frequency and intensity) in many areas of the world (IPCC 2021), possibly without significant changes in MAP.

The effect of water availability on vegetation depends not only on the amount and seasonality of precipitation, but also on soil properties (Rodríguez-Iturbe and Porporato 2005). Sandier soils allow deeper infiltration, promoting deeper root distributions, which may be associated with higher tree cover (Case and Staver 2018). Soil fertility has also been recognized as an important determinant of forest and savanna distribution at different spatial scales, especially in regions with similar precipitation regimes (Lloyd and others 2015; Pellegrini 2016). Savannas are often associated with lower soil fertility than forests (for example, low cation exchange capacity, organic matter, and macro- and micronutrients; Lloyd and others 2009). However, it is still unclear whether these differences in soil fertility are a cause or, rather, a consequence of forest–savanna distribution (Pellegrini 2016; Archibald and others 2019) and their effects vary depending on climate (Lehmann and others 2011).

Forest–savanna transition is not only determined by vegetation–climate–soil interactions but, also, by feedbacks with other factors such as fire, mainly in more mesic climates (Hoffmann and others 2012; Bernardino and others 2022). Specifically, fire–vegetation feedback in savannas allows frequent burning that, in turn, maintains a savanna (open-canopy) structure, where both climate and soil properties would predict the occurrence of a forest (closed canopy; Newberry and others 2020). Fire decreases tree cover, which subsequently favors light-dependent grass, promoting fuel for fire spread, and maintaining an open-canopy state (Bernardino and others 2022). However, the role of fire (either of natural or anthropogenic origin) as a determinant of forest–savanna transition is not fully understood (Veenendaal and others 2018), particularly for more mesic climates (Archibald and others 2019).

In South America, proxies of water availability such as MAP, precipitation seasonality, or mean precipitation in the dry season have a lower explanatory potential for tropical forest and savanna distribution than they do in Africa or Australia (Staver and others 2011; Lehmann and others 2014; Zeng and others 2014; Xu and others 2018). Indeed, there are extensive areas of savanna in tropical South America with MAP levels at which forest would be expected in Africa or Australia (Lehmann and others 2011, 2014). This suggests a different climatic control on the distribution of South American tropical forests and savannas. In addition, South American savannas differ from African or Australian savannas in other fundamental factors, such as soil properties and fire regime (Staver and others 2011), highlighting biogeographic differences among continents. These biogeographic differences can also occur within continents, as is the case of the two more extensive savanna regions in South America: the Cerrado (South of the Amazon region in Brazil) and the Llanos (north of the Amazon region between Colombia and Venezuela). Although both regions have a forest–savanna transition, they exhibit noticeable ecological differences, including vegetation structure and composition, and climatic and edaphic properties (Borghetti and others 2019), leading to different relationships between vegetation and the environmental factors that describe the transition. For example, the climatic space—a set of climate-related variables ranges—of the Cerrado forest–savanna transition (MAP $<$ 1500 mm, and the Maximum Climatological Water Deficit, MCWD < -300 mm; Malhi and others 2009) would predict forest for most of the Llanos savannas (see first part in the discussion section). This discrepancy indicates the importance of refining our understanding of the factors, relationships, and mechanisms that control the forest–savanna transition at the regional scale, to improve projections of global change effects on ecosystem distribution (Oliveras and Malhi 2016; Archibald and others 2019).

This study examines the climate, soils, and disturbance spaces of the forest–savanna transition between the Llanos ecoregion and northwestern Amazon forest in northern South America using remotely sensed data. We use several vegetation structure descriptors as indicators of forest–savanna occurrence and transition. We use multiple seasonal (length of dry season) and intra-seasonal (frequency and intensity of daily precipitation for the dry season) precipitation metrics, soil silt content, and fire frequency as explanatory variables for the transition. We hypothesize that: (1) fire frequency and intra-seasonal precipitation, particularly precipitation frequency during the dry season, have a more significant effect on the forest–savanna transition, whereas soil properties have a marginal effect; and (2) savannas in the Llanos occur in a climatic space (for example, MAP and MCWD) typical of forests in other tropical forest–savanna transition regions.

Methods

Study Area

The study area is located in northern South America, which corresponds to the Llanos ecoregion between Colombia and Venezuela, including parts of the Amazon basin's northwesternmost portion (Figure 1). MAP ranges from 1000 to 1500 mm in the northern region near the Colombia–Venezuela border to 2500–3500 mm in the forest–savanna transition and forest areas in the south and southwest (Borghetti and others 2019). The climate in the region is seasonal, with a drier season that extends from 4 to 7 months between November and April–May. Although savannas are typically water-limited ecosystems, large savanna areas in the Llanos do not exhibit annual moisture deficit under average climatic conditions (aridity index greater than 1, Zomer and others 2008; Figure 1a).

The landscape of the Llanos includes several types of savanna formations (for example, permanently and seasonally flooded savannas and high plain savannas), riparian or gallery forests, palm-dominated forests, and wetland vegetation (Romero-Ruiz and others 2010). The major soil groups are highly weathered and nutrient-poor oxisols in the forest, and oxisols, ultisols, and inceptisols in the savanna (Romero-Ruiz and others 2010). Overall, the region has a shallow water table (WT $<$ 5 m), mainly over the permanently and seasonally flooded savannas as well as riparian forests (WT $<$ 2 m; Fan and others 2013). The occurrence of fires is high and relatively frequent (0.5 to 2.0 years recurrence; Borghetti and others 2019) in the savannas, mainly during the dry season (Armenteras and others 2005). However, although vegetation and climate largely relate to fire occurrence (Barreto and Armenteras 2020), a large portion of fires in the savanna is related to traditional management practices and cattle grazing (Armenteras and others 2005; Romero-Ruiz and others 2010).

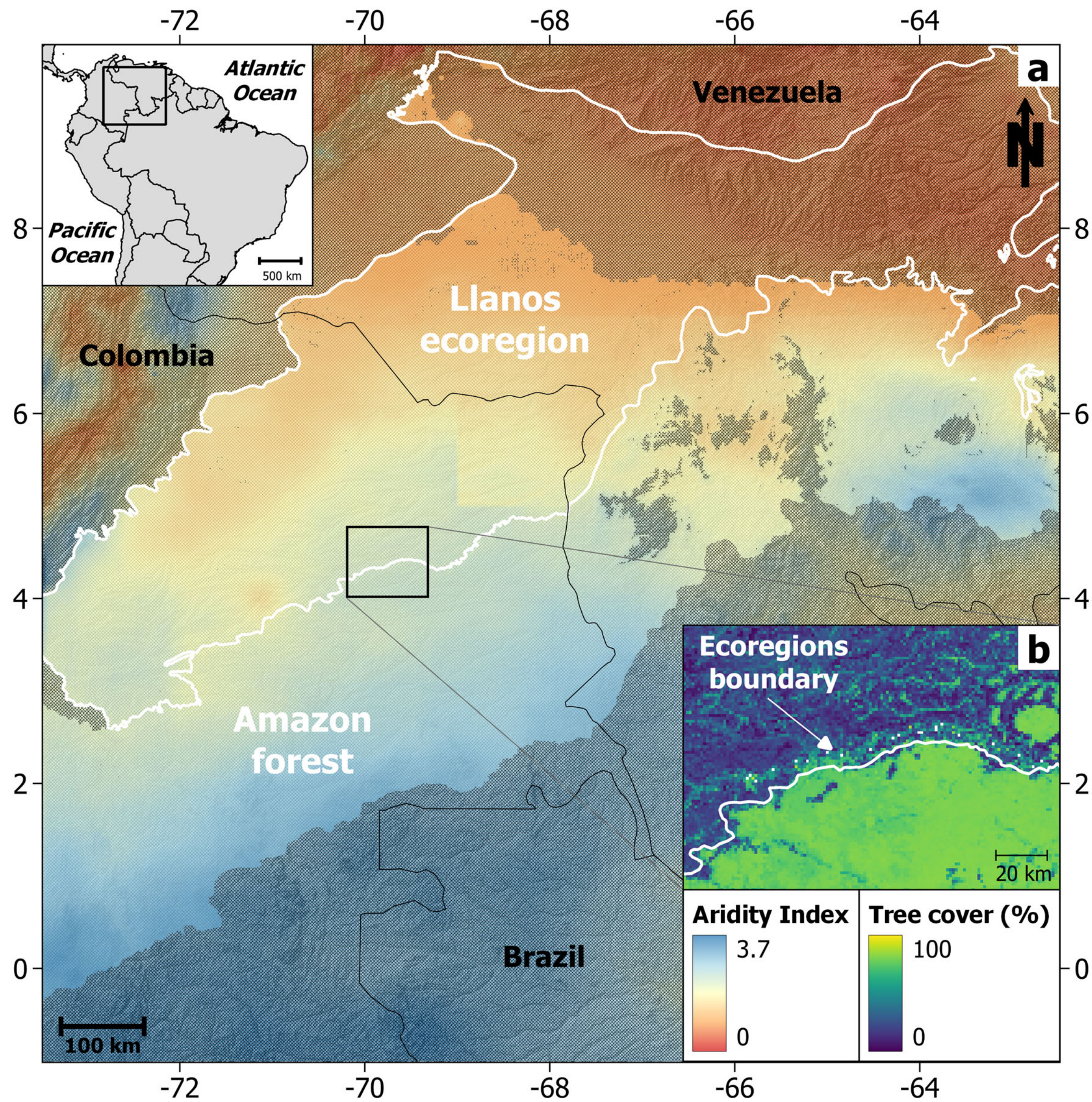

Figure 1. **a** Study area (highlighted pixels) in northern South America, showing Aridity index (AI) values, defined as the ratio of MAP to mean annual potential evapotranspiration (PET; Zomer and others 2008) The white line indicates the Llanos ecoregion boundary. Pixels outside the study area were excluded following the criteria described in Study Area Delimitation and forest–savanna Discrimination Section. MAP and PET data were obtained from CHIRPS (Funk and others 2015) and TerraClimate (Abatzoglou and others 2018) datasets for 1981–2010, respectively; hillshade was derived from SRTM (Jarvis and others 2008). **b** Percent tree cover for 2019 for an example area across the transition, derived from MODIS imagery, at 0.01° resolution (DiMiceli and others 2015).

Data Sources

We collected information on vegetation, climate, soil properties, fire, land cover, and topography from multiple remotely sensed data sources (Table 1). We obtained vegetation structure data from NASA's Global Ecosystem Dynamics Investigation (GEDI; Dubayah and others 2020) and the moderate-resolution imaging spectroradiometer (MODIS; DiMiceli and others 2015). Unlike MODIS, GEDI provides not only vegetation cover data, but also data on the vertical structure of vegetation, which is key to characterizing vegetation structural complexity and associated ecosystem processes (Stark and others 2020). From the GEDI dataset (collected between April 19, 2019, and September 02, 2020), we extracted canopy cover and the maximum Plant Area Volume Density ($PAVD_{max}$). PAVD is a measure of the vertical distribution of standing biomass (that is, the ratio between surface area and volume), including leaves, branches and trunk throughout the vertical profile of vegetation (Calders and others 2014; Marselis and others 2019; Dubayah and others 2020; Supporting Information S1). In this case, $PAVD_{max}$ is derived from the vertical profile of each GEDI pixel as a proxy of total vegetation structure (Meeussen and others 2020), with higher values for forest than for savanna vegetation. Finally, we obtained percent tree cover for 2019 from the MODIS Collection 6 Vegetation Continuous Fields product, at a 250 m resolution. All vegetation descriptors were gridded to 0.01° (~ 1.1 km) pixels, as described in Supporting Information S1 and Figure S1a.

For soils, we used a weighted average spanning three depth horizons (0–5 cm, 5–15 cm, and 15–30 cm) to obtain mean silt content for the top 30 cm of soil (Case and Staver 2018) from the SoilGrids dataset (Hengl and others 2017). We did not include other soil texture or fertility proxies due to their low Pearson (r) and Spearman (r_s) correlations ($<|0.25|$) with vegetation descriptors (Tables S1 and S2 in Supporting Information). We extracted burned areas from FIRECC51, a global monthly burned area product, over the 2001–2020 period (Chuvieco and others 2018). We excluded pixels with more than 50% invalid observations (that is, with a confidence level $\leq$ 70%) and calculated the number of times each pixel burned across the available period as an estimate of typical fire frequency (Lehmann and others 2014; Case and Staver 2018).

We used daily precipitation data from the Climate Hazards Group InfraRed Precipitation with Station data (CHIRPS; Funk and others 2015) available at 0.05° (~ 5.5 km) to calculate multiple precipitation statistics over 1981–2019. We selected CHIRPS due to its high spatial resolution and performance for our study region (Paredes-Trejo and others 2017; Valencia and others 2023 and Figure S11 in Supporting Information). For each CHIRPS pixel, we calculated mean annual precipitation (MAP, in mm), and the following seasonal and intra-seasonal precipitation metrics—this metrics have been referred to as precipitation variability by other authors (for example, Case and Staver 2018; Xu and others 2018; D'Onofrio and others 2019; Ritter and others 2020; Schwartz and others 2020)—for the dry season: mean total precipitation (MAP_d, in mm), mean daily precipitation intensity (α_d, in mm), mean frequency of wet days (λ_d), and mean season length (T_d, in days) with $MAP_d = \alpha_d \lambda_d T_d$. To define the dry season length, instead of setting an arbitrary precipitation threshold [for example,, months with monthly precipitation less than 100 mm (Anderson and others 2022) or months with potential evapotranspiration greater than precipitation (Yan and others 2016)], we used the global gridded dataset (Rainy and Dry Seasons, RADS, dataset) developed by Bombardi and others (2019). In their work, Bombardi and others (2019) defined the wet and dry seasons length based on the dates of the minimum and maximum first harmonic of the mean annual cycle of precipitation at each CHIRPS pixel. We estimated λ_d as the total number of wet days (daily precipitation > 0) in the dry season divided by the total dry season length (T_d). We analyzed several precipitation metrics for the dry season instead of for the wet season (for example, Good and Caylor 2011; Case and Staver 2018; Xu and others 2018; D'Onofrio and others 2019) because recent studies from our group highlight that precipitation in the dry season explains better the forest–savanna transition in our study area (Hoyos and others 2022). Additionally, all vegetation structure descriptors showed higher correlations with seasonal and intra-seasonal precipitation metrics for the dry season than for the wet season (Tables S2 and S3 in Supporting Information and Supporting Information S3). Finally, following Malhi and others (2009) and for comparison with our study, we calculated the Maximum Climatological Water Deficit (MCWD; Aragão and others 2007) based on the mean annual cycle of precipitation (1981–2019) with a fixed monthly evapotranspiration of 100 mm.

Although regional climatic patterns are reasonably well represented in a resolution of 0.05° (~ 5.5 km), vegetation structure in the forest–savanna transition may vary considerably over such distance. Because aggregation techniques could cause loss of vegetation structure variability (Hirota and others 2011; Figure S3 in Supporting Information), all data layers, except CHIRPS, were resampled to match the resolution of the GEDI data (0.01°) using bilinear interpolation in the projectRaster function of the raster R package (Hijmans 2020). We rescaled CHIRPS data to 0.01° by dividing each pixel at 0.05° into 25 pixels without varying the original values. All the datasets were converted into mean temporal values because our focus is on the average transition state. Maps of all variables are shown in Supporting Information Figure S4.

Study Area Delimitation and Forest–Savanna Discrimination

We limited our study area to pixels with an elevation lower than 800 m.a.s.l. and a minimum monthly temperature higher than 15 °C, to exclude Andean ecosystems and to avoid slope and aspect effects. To do this, we used elevation and temperature data from the Shuttle Radar Topography Mission (SRTM; Jarvis and others 2008) and WorldClim (Fick and Hijmans 2017) datasets, respectively. We also masked out pixels with more than 30% of the area covered by croplands, urban areas and water from ESA's 2019 global land cover map (ESA 2017; Table 1). Although riparian forests in the Llanos have different soil properties and water table depths (water availability) compared to the grasslands, we did not exclude the former as they represented less than 5% ($N = 4740$) of the total pixels in the study area.

Savannas can be seen as having a mesic boundary where they transition into forests and an arid boundary where they transition into arid vegetation (Archibald and others 2019). Hence, the datasets were split into arid and mesic transitions using the Aridity Index (AI), which captures the interactive effects of climate on plants' water availability (Pellegrini 2016). Given our interest in the mesic transition, we masked out pixels with AI < 1 to exclude savanna regions with an annual moisture deficit under average climatic conditions (Figure 1). To reduce sample size effects, we selected an equivalent area within the forest ecoregion to obtain a similar number of pixels in both ecosystems. In addition, to focus the analysis on forest and savanna vegetation, we defined pixels as forest or savanna based on canopy cover (savanna < 40% and forest ≥ 40%), tree cover (savanna < 60% and forest ≥ 60%), and $PAVD_{max}$ (savanna < 0.10 m^2/m^3 and forest ≥ 0.10 m^2/m^3; further details and supporting information for these thresholds in Supplementary Information S1). Finally, all datasets were extracted at 0.01° resolution for GEDI available pixels ($N = 201{,}474$; Figure S3 in Supporting Information).

Spatial Analysis of the Forest–Savanna Transition

We looked for spatial patterns in vegetation structure descriptors and predictor variables across 1835 transects perpendicular to the forest–savanna transition and separated by ~ 1.1 km. We sampled transects in adjacent 0.01° available pixels (details in Supplementary Information S2 and Figure S5a in Supporting Information). Pixels in each transect were numbered sequentially from 1 in the forest to 580 in the savanna (even as the total length of each cover type varied among transects) to calculate the median and the 10th, 25th, 75th, and 90th percentiles across transects (Figure S4b in Supporting Information).

Statistical Analysis

We analyzed the relationship between vegetation descriptors (that is, canopy cover, tree cover, and $PAVD_{max}$) and the selected predictor variables using generalized linear models (GLMs; McCullagh and Nelder 1989). We standardized the predictor variables by subtracting the mean and dividing by the standard deviation. Hence, each variable's coefficient magnitude measures its importance in the model. The goodness of fit was evaluated as the fraction of deviance explained (pseudo-R^2, R^2 henceforth for brevity), equivalent to the explained variance in a linear least-squares regression model. It was computed as $R^2 = 1 - D_m/D_0$, where D_m is the residual deviance, that is, the deviance that remains unexplained by the fit, and D_0 is the deviance of the intercept-only model (D'Onofrio and others 2019). To consider the potential effect of differences in spatial variability between precipitation metrics (0.05°) and other predictor and response variables (0.01°, see data sources section), we fitted 1000 GLMs using stratified random samples of 5% ($N = 10{,}074$) of the available 0.01° pixels to determine the direction, strength, and significance of predictor variables on tree cover, canopy cover, and $PAVD_{max}$. See Supporting Information S4 for further details. All statistical analyses were performed in R (R Core Team 2022).

Results

Forest–Savanna Transition

Our results show, as expected, significant changes in vegetation structure across the forest–savanna transition (Figure 2a–c). Tree cover exhibits the most abrupt change compared to canopy cover and PAVD, while the large 10th–90th and 25th–75th percentile ranges indicate variations in vegetation structure in both forest- and savanna-dominated regions as well as along the transition.

Transect patterns show that although MAP_d and λ_d are highly correlated with vegetation descriptors (r_s and $r \geq 0.54$; Supporting Information Tables S1 and S2), both variables exhibit a more gradual (Figure 2d, e) transition than canopy cover, tree cover, or $PAVD_{max}$ (Figure 2a–c). Overall, MAP_d and λ_d are higher in the forest than in the savanna, with median values of $MAP_d = 953$ mm and λ_d=0.38 in the forest, and of $MAP_d = 360$ mm and λ_d=0.19 in the savanna. The spatial variability (that is, 10th–90th and 25th–75th percentile ranges) of

Table 1. Description of Data and Sources Used in the Study

Category	Variables	Dataset	Spatial resolution	Temporal resolution	Temporal coverage	Reference
Vegetation	Tree cover (%)[a]	MODIS	0.25 km	Annual	2000–present	DiMiceli and others (2015)
	Canopy Cover (%)[b] Maximum Plant Area Vegetation Density ($PAVD_{max}$, m^2/m^3)	GEDI	0.025 km	Variables (depends on the ISS trajectories)	2019–present	Dubayah and others (2020)
Soil properties	Sand, clay, and silt content (%) Cation exchange capacity (CEC, mmol(c)/kg) Soil organic carbon (SOC, dg/kg)	SoilGrids v2.0	0.25 km	–	–	Hengl and others (2017)
Fire	Burned area	FIRECCI51	0.25 km	Monthly	2001–2020	Chuvieco and others (2018)
Climate	Mean annual precipitation (MAP, mm) Funk and others (2015)	CHIRPSv2.0	0.05°	(~ 5.5 km) Mean total precipitation in dry (*d*) season (MAP_d, mm) Mean length of dry (d) season (T_d, days) Mean daily precipitation intensity in dry (*d*) season (α_d, mm/day)	Daily	1981–present
		Mean daily precipitation frequency in dry (*d*) season (λ_d)				
	Monthly minimum temperature (°C)	WorldClim v2.1	~ 1.0 km	Monthly	1970–2000	Fick and Hijmans (2017)
Potential evapotranspiration (PET, mm)	TerraClimate	~ 4.0 km	Monthly	1981–2010	Abatzoglou and others (2018)	
Land cover	Global land cover	ESA	0.30 km	Annual	1992–present	ESA (2017)
Topography	Elevation	SRTM	0.25 km	–	–	Jarvis and others (2008)

[a]The percent tree cover refers to the amount of skylight obstructed by tree canopies equal to or greater than 5 m in height (DiMiceli and others 2015); [b]The GEDI-derived canopy cover is the percent of the ground covered by the vertical projection of canopy material (that is, leaves, branches and stems only).
MODIS Moderate resolution imaging spectroradiometer, GEDI Global ecosystem dynamics investigation, ISS International space station, SoilGrids Global gridded soil information, FIRECCI51 the ESA FireCCI project, CHIRPS Climate Hazards Group InfraRed Precipitation with Station data, ESA European Space Agency, SRTM Shuttle radar topographic mission.

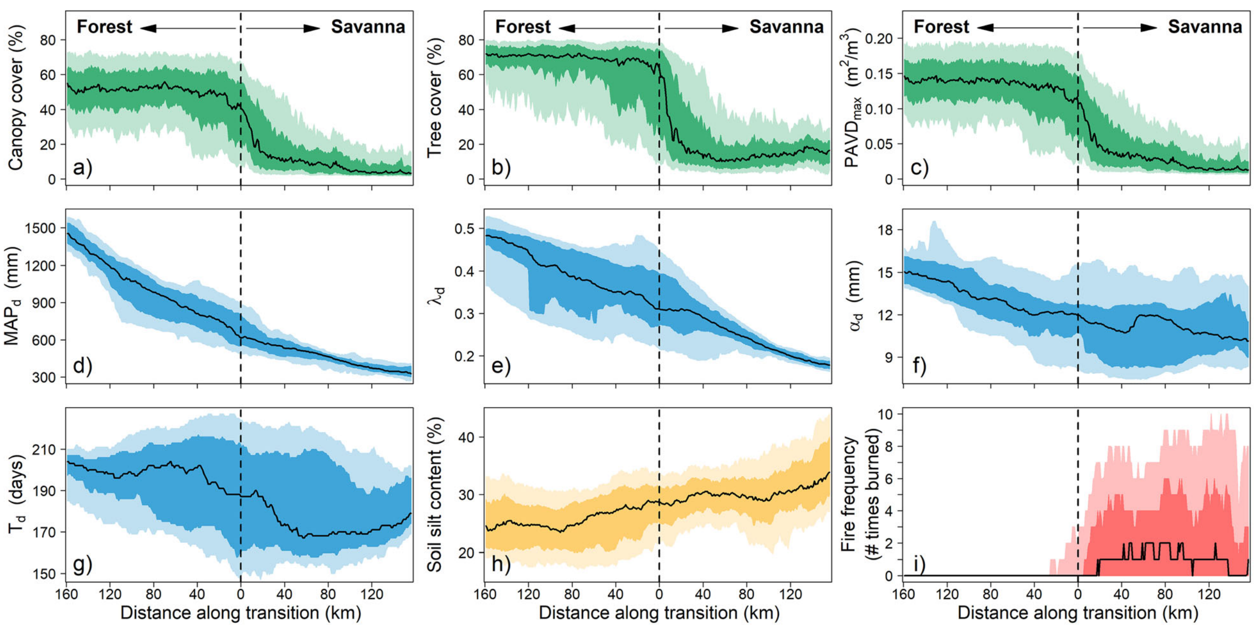

Figure 2. Changes in vegetation structure (**a**–**c**), climate (**d**–**g**), soil (**h**), and fire (**i**) variables across the forest–savanna transition. **a** Canopy cover, **b** tree cover, **c** maximum Plant Area Volume Density (PAVD$_{max}$), **d** mean total dry season precipitation (MAP$_d$), **e** frequency of wet days (precipitation > 0) within the dry season (λ_d), **f** intensity of wet days within the dry season (α_d), **g** length of the dry season (T_d), **h** soil silt content, and **i** fire frequency. The boundary between forest and savanna (vertical dashed line) along the transect is located where the mean of canopy cover, tree cover, or PAVD$_{max}$ (solid black line) crosses the forest–savanna threshold. In all panels, the lightest shaded band represents the 10th–90th percentile, the darker shaded band is the 25th–75th percentile, and the black line represents the median (50th percentile) for all transects (n = 1835). Supporting Information Figure S8 shows results for predictor variables that were not considered for further analysis.

MAP$_d$ and λ_d is highest near the transition and decreases toward the initial (forest) and final (savanna) transect sections, particularly in the latter (Figure 2d, e and Supporting Information Figure S4d, e). Although α_d and T_d also decrease over the transition (Figure 2f, g), they do not show evident differences in median or percentile ranges between forest (α_d=13.05 mm/day; T_d = 199 days), nor savanna (α_d=10.35 mm/day; T_d = 178 days). This indicates that precipitation frequency (instead of dry season length or precipitation intensity) explains the difference in MAP$_d$ between forest and savanna (Figure 2d).

Similar to α_d and T_d, soil silt content also exhibits small changes in the median or percentile range over the transition (Figure 2h), consistent with low correlation values (r and r_s <|− 0.28|; Tables S1 and S2 in Supporting Information). Fire frequency is highly correlated with vegetation descriptors (r and r_s >|− 0.51|) and is the only predictor variable that shows a sharp transition (Figure 2i), similar to the vegetation descriptor variables. Fire frequency reaches its highest values in the savanna while it is close to zero in the forest. However, there is a large spatial variability (that is, 10th–90th and 25th–75th percentile ranges) in fire frequency in the savanna (Supporting Information Figure S3i). These results coincide with several studies that report that savanna occurs more commonly where fires are present (Lehmann and others 2011; Staver and others 2011; Bernardino and others 2022).

Forest–Savanna Transition Climatic Space

We plotted MAP versus the selected predictor variables to analyze the ranges in which forest and savanna occur in the Llanos region (Figs. 3 and S9 in Supporting Information). We used canopy cover (solid line), tree cover (dotted line), and PAVD$_{max}$ (dashed line) to define the forest and savanna climatic spaces. We selected MAP as the independent variable because it has been widely used to analyze the global (or regional) distribution of forest and savanna in the tropics (for example, Staver and others 2011; Xu and others 2018). The results show that instead of a single threshold in seasonal and intra-seasonal precipitation metrics during the dry

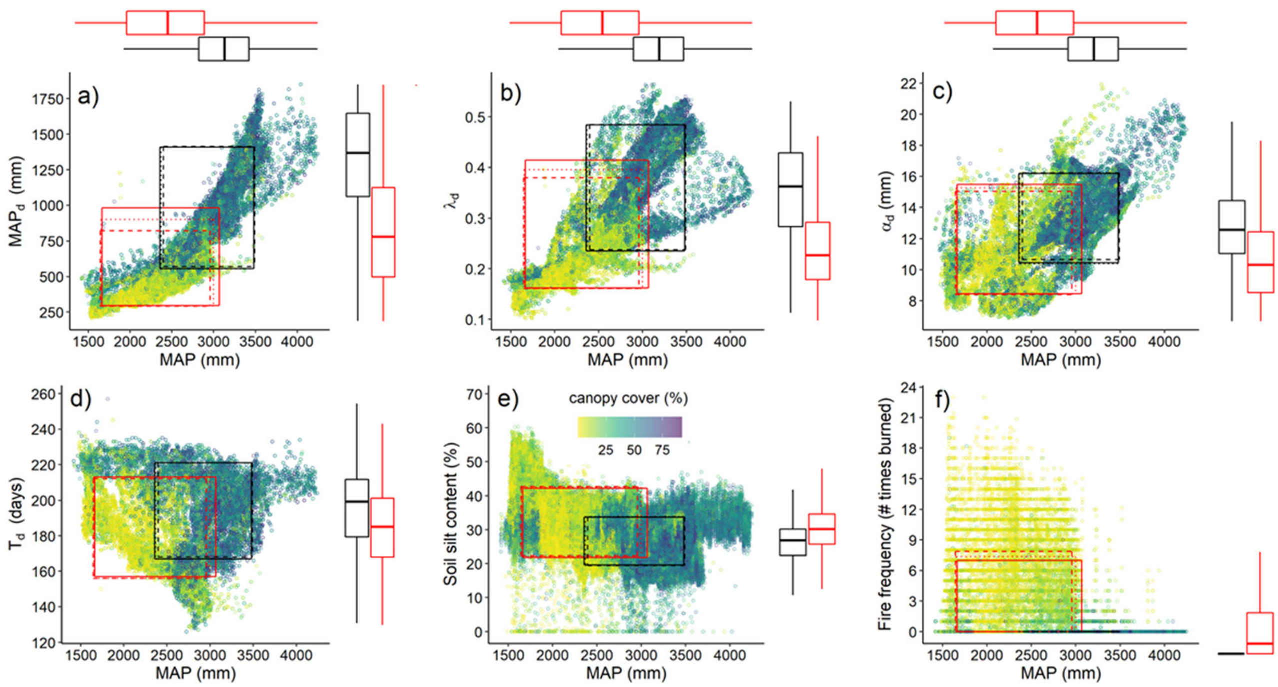

Figure 3. Climate space of forest and savanna based on mean annual precipitation (MAP) and **a** mean total dry season precipitation (MAP_d), **b** frequency of wet days (precipitation > 0) within the dry season (λ_d), **c** intensity of wet days within the dry season (α_d), **d** length of the dry season (T_d), **e** soil silt content (%), and **f** fire frequency. Boxes indicate each variable's 10th and 90th percentiles for savanna (red) and forest (black) as defined by canopy cover (solid line), tree cover (dotted line), and $PAVD_{max}$ (dashed line). Boxplots show the values of each variable for all savanna (red) and forest (black) pixels defined by canopy cover.

season and in the soil silt content (Figure 3a–e), there is a broad range of values in each variable in which both savanna and forest can occur. Notably, fires occur almost exclusively in the savanna (Figure 3f), with scattered fire pixels occurring in the forest. However, 46% of savanna pixels (N = 53,271) did not have any fires in the period of 2001–2019. Further, these ranges are similar regardless of the variable used to define savanna and forest (that is, canopy cover, tree cover, and $PAVD_{max}$; Figure 3). This indicates that fire occurrence is not an intrinsic property of savannas in this region.

Forest occurs in pixels with MAP > 2360 mm, while savanna occurs in MAP levels between 1665 and 3070 mm, indicating that both are present between 2360 and 3070 mm (Figure 3a). However, pixels with similar MAP exhibit different canopy cover values depending on precipitation frequency and/or intensity. For example, in the MAP overlap range, savanna occurs if MAP_d and λ_d are lower than 556 mm and 0.23, respectively (Figure 3a, b). However, MAP_d and λ_d also exhibit a broad range of values in which both forest and savanna can occur (556 mm $\leq MAP_d \leq$ 981 mm and 0.23 $<\lambda_d<$ 0.41). α_d and T_d show lower variability and a larger overlap between forest (10.4 mm/day $<\alpha_d<$ 16.2 mm/day; 167 days $< T_d <$ 221 days) and savanna (8.5 mm/day $<\alpha_d<$ 15.5 mm/day; 157 days $< T_d <$ 213 days) in their 10th–90th percentile ranges than for MAP_d and λ_d (Figure 3c, d), consistent with results shown in Figure 2f, g. Indeed, both forest and savanna can occur when α_d and T_d vary between 10.4 mm/day $<\alpha_d<$ 15.5 mm/day and 167 days $< T_d <$ 213 days, respectively.

Soil silt content shows little difference between savanna and forest (Figure 3e). Overall, the savanna dominates in pixels with higher soil silt content (21.8–42.2%) than the forest (19.6–33.7%), with an overlap range between ~ 22 and ~ 34%.

Determinants of the Forest–Savanna Transition

Our GLM results show that all selected predictor variables, except for soil silt content, have a statistically significant effect on canopy cover (Figure 4). In particular, models explain between 52.2 and 55.4% of the data deviance (Table S3 in Supporting Information). Fire frequency followed by λ_d are the most important predictor variables for canopy cover, as

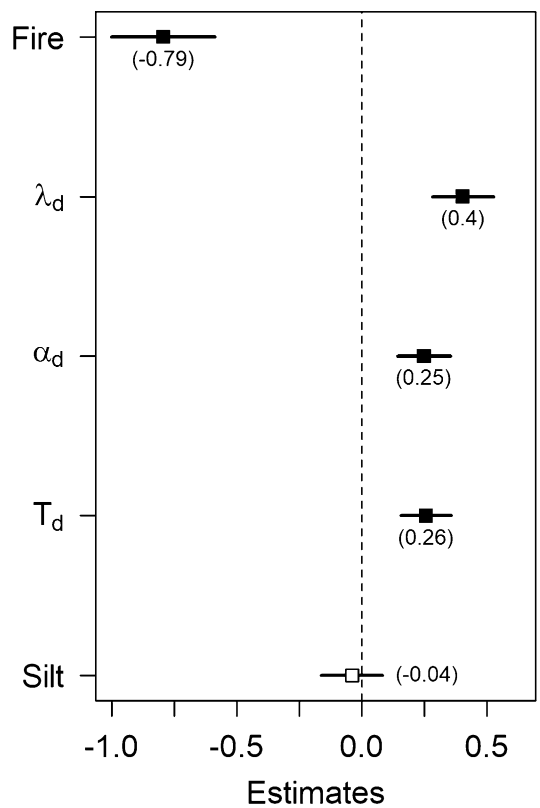

Figure 4. Effect of each predictor variable on canopy cover. Predictor variables were standardized such that their GLM coefficient magnitude is a measure of their importance in the model. The median estimate (values in parentheses) and 95% confidence interval (error bars) are based on 1000 GLMs (see statistical analysis section and Supporting information S4). Terms are not significant (open symbol) when the confidence interval includes zero (dashed vertical line). Predictor variables are: fire frequency (fire), mean daily precipitation frequency in dry season (λ_d), mean daily precipitation intensity in dry season (α_d), mean length of dry season (T_d), soil silt content (silt). See Supporting Information Figure S10 for equivalent analyses with tree cover and $PAVD_{max}$, and Supporting Information Table S3 for details of GLMs results.

indicated by the magnitude of standardized estimates for both variables, with fire frequency having a negative effect on canopy cover, while λ_d having a positive effect ($-$ 0.79 and 0.40, respectively). Given the direct association between the seasonal and intra-seasonal precipitation ($MAP_d = \lambda_d \alpha_d T_d$), when α_d and T_d are held constant, the increase of λ_d corresponds with an increase in MAP_d that results in increased canopy cover. Consequently, canopy cover and λ_d are higher in areas with higher MAP_d (Figs. 2 and 3; Supporting Information Figure S4). Although α_d and T_d are also statistically significant, they have lower explanatory power. Finally, soil silt content has the lowest and non-statistically significant effect on canopy cover. Models of tree cover or $PAVD_{max}$ as dependent variables show similar magnitude and significance of standardized estimates (Table S3 and Figure S10 in Supporting Information), although λ_d (0.48) shows a slightly higher explanatory power than fire frequency ($-$ 0.42) for the tree cover model. These results highlight the importance of using multiple descriptors when assessing structurally diverse ecotones such as the forest–savanna transition.

Discussion

Beyond a MAP Threshold for Characterizing the Forest–Savanna Transition in the Llanos

Multiple thresholds, mainly based on MAP, have been suggested to define tropical forest and savanna distribution at regional (Malhi and others 2009; Ciemer and others 2019), continental (Good and Caylor 2011; Lehmann and others 2011; Staal and others 2020), and global scales (Staver and others 2011; Archibald and others 2019). Our results show that there is a broad MAP range where both forest and savanna occur in northern South America (2360–3070 mm, Figure 4a), which is higher than previously proposed for this region (1200–2100 mm; Ciemer and others 2019; Staal and others 2020) as well as globally (1000–2500 mm; Staver and others 2011). This indicates that savannas in the Llanos occur at MAP ranges typical of forests in other South American regions (for example, the Cerrado, Figure 5) and elsewhere. Indeed, the climatic space for savannas in the Llanos region does not correspond to the predicted climate space (MAP and MCWD) for savannas in the Cerrado region proposed by Malhi and others (2009); yellow portion of Figure 5; $MAP < 1500$ mm and $MCWD < -300$ mm. A comparison between the forest–savanna transition in the Llanos and that in the Cerrado regions show that in the former, the savanna occurs under MAP and MCWD regimes that would be associated with forest in the latter (Figure 5b). In the Llanos region, for instance, forest occurs in pixels with $MAP > 2360$ mm and $MCWD > -230$ mm, but there is a large overlap region with savannas which also occur at high MAP (up to 3070 mm) and low dry season severity (up to 33 mm) (Figure 5a; that is, more negative MCWD values indicate a larger water deficit). In consequence, our results suggest that the commonly used MAP threshold of 1500 mm/y for the forest–savanna-like ecosystem transition (for example, Li and others 2022) could

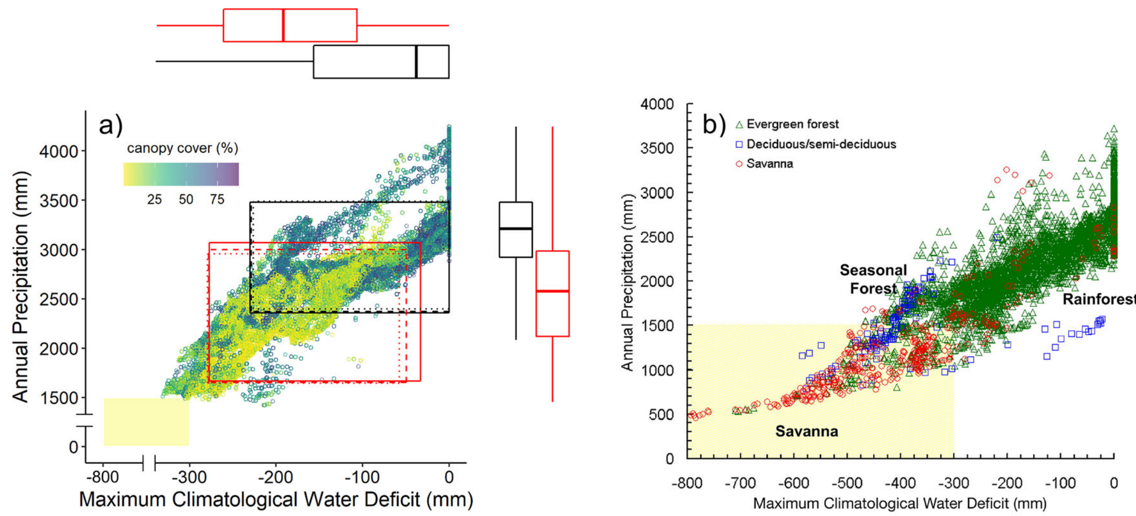

Figure 5. Relationship between **a** canopy cover and climatic space (MAP, MCWD) for the forest–savanna transition in the Llanos region, **b** vegetation type and climate space for the Cerrado region (0°–20°S and 45°W–70°W) modified from Malhi and others 2009. Boxes in **a** indicate each variable's 10th and 90th percentiles for savanna (red) and forest (black) as defined by canopy cover (solid line), $PAVD_{max}$ (dashed line), and tree cover (dotted line). Boxplots show the MAP and MCWD values for all savanna (red) and forest (black) pixels defined by canopy cover. The light yellow-filled area in both panels represents the MAP (< 1500 m) and MCWD (< − 300 mm) ranges dominated by savannas according to Malhi and others (2009).

underestimate regional forests' climate-tipping point.

Forest and savanna occur in a wide range of dry season precipitation metrics (Figure 3a–d). Our results suggest that there are MAP levels in which forest (> 3070 mm) and savanna (< 2360 mm) dominate regardless of the values of other variables (λ_d, α_d, T_d, or MAP_d; Figure 3 and Figure S9 in Supporting Information). However, regions with similar MAP but different dry season seasonal or intra-seasonal precipitation exhibit different canopy cover values (Figure 3). Indeed, various combinations of mean dry season lengths, precipitation frequency, and intensity can result in a similar MAP or MAP_d. For example, at intermediate MAP (2360–3070 mm), our results show that savanna (forest) occurs if λ_d and α_d are lower (higher) than 0.23 and 8.5 mm/day (0.41 and 15.5 mm/day), respectively. These results highlight that the current and future definition of forest and savanna distributions requires additional considerations of a climatic space with multiple precipitation characteristics, as suggested by Schwartz and others (2020).

Dry Seasonal Precipitation as a Determinant of Forest–Savanna Transition

Our statistical analysis reveals that seasonal and intra-seasonal precipitation for the dry season, particularly precipitation frequency (λ_d), are significant predictors of vegetation in the forest–savanna transition (Figure 4 and Supporting Information Table S3). More specifically, although we did not assess the effects of precipitation variability on canopy cover for different MAP windows, our results suggest that intra-seasonal precipitation can be more important at intermediate MAP levels (that is, 2360–3070 mm) in which both forest and savanna can occur (Figure 4a–d), as indicated by Xu and others (2018) for MAP between 500 and 1500 mm in the global tropics. Our results are consistent with previous studies showing that seasonal and intra-seasonal precipitation is a key determinant of forest and savanna dynamics and their distribution at local and global scales (for example, Good and Caylor 2011; Case and Staver 2018; Xu and others 2018). However, in contrast to those studies, our analysis indicates that seasonal and intra-seasonal precipitation during the dry season dry season are more important than for the wet season in explaining the transition (Supplementary Tables S1 and S2), consistent with Zeng and others (2014) and Hoyos and others (2022) for tropical South America and north–west South America, respectively.

Overall, our results show that canopy cover increases when daily precipitation is more frequent and intense (Figure 3b–c). Hoyos and others (2022) show how shorter dry spells during the dry season increase the probability of forest occurrence in Northwest South America. In addition, Good and Caylor (2011) and Xu and others (2018) show that tree cover is also higher in areas where precipitation is more frequent but less intense, evidencing that the tropical vegetation response to precipitation frequency and intensity is heterogeneous and varies regionally according to differences in seasonality and water-use strategies between grasses (savanna) and trees (forest) (Case and Staver 2018).

Although sandier soils can help to explain increases in canopy cover with precipitation intensity in African savannas (for example, Case and Staver 2018), we did not observe differences in soil texture (indicated by silt content) between forest and savanna (Figure 3e and Supporting Information Figure S4). Additionally, silt content does not significantly affect canopy cover, tree cover, nor $PAVD_{max}$ (Figure 5 and Figure S10 in Supporting Information). Our analysis suggests that soil properties (both texture and fertility, which was not significant to be included in our analysis) do not provide an alternative mechanism to explain the forest–savanna transition compared to intra-seasonal precipitation in the Llanos (Tables S1 and S2 in Supporting Information). This is consistent with the results of Hoyos and others (2022), who highlight the low explanatory power of soil units on the probability of forest occurrence in the Llanos, which may be related to similar long-term climate, parent material, and relief across the transition. However, global soil databases may be insufficiently accurate or fine-scaled to represent differences in soil properties between forest and savanna and among savanna types (that is, permanently and seasonally flooded savannas and high plain savannas) in the Llanos region, which require further analysis.

Savannas occur more commonly than forests in regions with longer dry seasons (T_d) (Archibald and others 2019; Jaramillo 2023). However, our results show that despite the low explanatory power of T_d (Table S3 in Supporting Information), it has a positive effect on canopy cover (Figure 5 and Figure S10 in Supporting Information). This suggests that a long dry season is not necessary for the occurrence of savanna, consistent with Staver and others (2011) for South America, highlighting how the precipitation distribution within the dry season may be more important than its duration.

The Role of Fire Frequency on Transition

Our results coincide with several studies reporting that fire is one of the most important factors explaining current (Staver and others 2011; Xu and others 2018; Newberry and others 2020) and past (Sato and others 2021) distribution of forest and savanna. Fire–vegetation feedbacks in savannas allow frequent burning that maintains an open-canopy where both climate and soil could otherwise support forest, consistent with the idea of a fire-suppression threshold (Hoffmann and others 2012; Bernardino and others 2022; Holdo and Nippert 2023). This can help to explain the co-occurrence of savanna and forest pixels in the same climatic space or soil silt content (Figure 4a–e). Indeed, savanna occurs more commonly where fires are present (for example, Lehmann and others 2011; Staver and others 2011; Bernardino and others 2022; Figs. 2i and 3f), perhaps as a consequence of its biomass being more flammable, which explain the importance of fire frequency predicting the transition in our analysis (Figure 4). However, our results also indicate that 46% of the savanna pixels ($N = 53{,}271$) did not have fires in our study period between 2001 and 2019 (Figure 3f and Figure S4i in Supporting Information). More interestingly, between 30 and 42% of savanna pixels that share the same climatic space of forest pixels do not have fires for this period (Supporting Information Figure S12). Thus, our results suggest that fire frequency alone does not explain the present-day occurrence of savanna pixels in the same climatic or edaphic space of forest in the Llanos region. This shows that, despite the key role of fire occurrence to determining forest–savanna transition in mesic regions (for example, our results and Lehmann and others 2011, 2014; Staver and others 2011; Xu and others 2018; Holdo and Nippert 2023), it is required to advance in the relationship between vegetation and fire to separate cause from effect (Jaramillo 2023). Further understanding of not only fire occurrence but also functional characteristics that may increase (or decreased) fire proneness is required. These characteristics include, flammability, dry matter content, presence of flammable resins, and more generally functional traits associated with fire (Armenteras and others 2021; Meza and others 2023).

Our results also show that fires in the savannas of the Llanos occur in pixels with MAP levels (> 2000 mm, Figure 3f), where fires are unlikely for other savanna regions (Lehmann and others 2011), evidencing the biogeographic differences between the Llanos and other savannas (Romero-

Ruiz and others 2010). Most fires in the Llanos occur during the dry season (November to April–May) and are mostly associated with human activities, such as traditional agricultural practices and cattle grazing (Armenteras and others 2005, 2020; Romero-Ruiz and others 2010). More specifically, Barreto and Armenteras (2020) show that vegetation (indicated by NDWI) followed by mean monthly temperature and human alteration are the most important variables predicting fire occurrence in the Llanos ecoregion. This key role of human activities in present-day fire regimes has also been documented in the Cerrado and African savannas via fire ignition or suppression. Burned area products are among the best data sources to estimate fire frequency at regional and global scales (Lizundia-Loiola and others 2020). However, they have a limited time coverage, which precludes the identification of fires with long return intervals ($>$ 20 years) and potentially relates to the absence of fires in some savanna pixels.

Alternative Determinants of Forest–Savanna Transition

Some regions with high water and nutrient availability can result in open-canopy conditions (for example, savanna) independent of the fire regime (Archibald and others 2019). This may also explain the presence of savanna pixels without fires in the same climatic or edaphic space of forest in our study area (Figs. 4 and S12 in Supporting Information). For example, seasonal flooding during the wet season is common in some savanna regions of the Llanos (Borghetti and others 2019). Indeed, seasonal flooding decreases tree cover in mesic regions such as the Llanos as waterlogging can create anoxic conditions and limit forest seedling establishment in the savanna (Oliveras and Malhi 2016; Daskin and others 2019). However, although a preliminary analysis confirms that some savanna pixels show high water occurrence (Figure S13a in Supporting Information), only $\sim$ 2% ($N = 560$) of savanna pixels in the same climatic or edaphic space of forest also exhibit water occurrence in the period 1984–2020 (Supporting Information Figure S13b). Additionally, forest and savanna regions that share the same climatic space have a similar water table depth (Figs. S14 and S15 in Supporting Information). Therefore, alternative factors that may contribute to explaining forest–savanna transition in the Llanos and require further exploration include: (i) plant rooting depth (Langan and others 2017); (ii) tree–grass competition (Xu and others 2018); (iii) human activities via agriculture (Berrio and others 2012); (iv) herbivory (Dantas and Pausas 2022); and (v) atmospheric CO_2 concentration (Sato and others 2021).

Concluding Remarks

The forest–savanna transition can be particularly sensitive to environmental change (Oliveras and Malhi 2016). To predict the response of these ecosystems to local (for example, fire regime) and global (for example, climate change) changes, it is essential to understand the factors and relationships explaining the distribution of forest and savanna at multiple spatial scales. Our results show that savannas in the Llanos ecoregion occur at MAP values ($>$ 1500 mm) that would be associated with forest in other savanna regions (for example, the Cerrado). In addition, the MAP range where both ecosystems can occur (2360–3070 mm) is higher than the ones reported for other forest–savanna transition regions. This highlights the biogeographic differences among savannas regions around the world. Additionally, these results suggest that typical MAP thresholds (for example, Malhi and others 2009) can overestimate the tropical forest distribution. Notably, our results highlight how the response of the forest–savanna transition to environmental change (for example, climate-tipping points) can be different between the northern (that is, Llanos) and southern (that is, the Cerrado) Amazon region. In addition, our analysis points to the importance of fire frequency and daily precipitation frequency for the dry season on the forest–savanna transition. Accordingly, future projections of forest and savanna dynamics and distribution should consider not only MAP changes (for example, Ciemer and others 2019; Staal and others 2020) but also changes in seasonal and intra-seasonal precipitation variability and fire-vegetation feedback. This is particularly important for Northern South America, where climate projections show, with high confidence, an increase in dry days (that is, lower precipitation frequency) and drought frequency (IPCC 2021). Finally, our results contribute to further understanding the factors, relationships, and mechanisms behind the forest–savanna transition at regional scales, which are needed to assess the environmental change effects on this ecologically, biogeochemically, and climatically important ecotone.

ACKNOWLEDGEMENTS

The authors thank Catalina González (Universidad de los Andes) and Carlos Jaramillo (Smithsonian

Tropical Research Institute) for their comments on an earlier version of this manuscript. The authors are also grateful to Diana María Agudelo (Universidad de Antioquia) and Alex Correa-Metrio (Universidad Nacional Autónoma de México) for their support with the statistical analysis. This work was funded by the Universidad de Antioquia through the Estudiante Instructor Program for graduate studies and the Colombian Ministry of Science, Technology and Innovation (MINCIENCIAS) through program ''Sostenibilidad de sistemas ecológicos y sociales en la cuenca Magdalena-Cauca bajo escenarios de cambio climático y pérdida de bosques'' (code 1115-852-70719) with funds from ''Patrimonio Autónomo Fondo Nacional de Financiamiento para la Ciencia, la Tecnología y la Innovación, Fondo Francisco José de Caldas''. DA was funded by the Universidad Nacional de Colombia - UNAL and the Sistema Nacional de Regalías – SNR in the framework of the project ''Diseño participativo de estrategias para la reducción de incendios forestales, la conservación de la biodiversidad y el desarrollo regional en paisajes multifuncionales de Vichada (BPIN 2020000100456)''.

FUNDING

Open Access funding provided by Colombia Consortium.

DATA AVAILABILITY

The original data used in this study are all publicly available from their sources: MODIS: https://ladsweb.modaps.eosdis.nasa.gov/, SoilGrids: https://soilgrids.org/, GEDI: https://gedi.umd.edu/, SRTM: https://srtm.csi.cgiar.org/srtmdata/, Terralimate: http://www.climatologylab.org/terraclimate.html, and ESA: http://maps.elie.ucl.ac.be/CCI/viewer/download.php. The MCWD data can be produced using data from CHIRPS combined with code available from Campanharo and Silva-Junior (2019) at: https://doi.org/10.5281/zenodo.2652629. The dataset that supports the findings of this study will be available through a data-sharing repository (for example, Zenodo).

REFERENCES

Anderson LO, Burton C, dos Reis JBC, Pessôa ACM, Bett P, Carvalho NS, Junior CHLS, Williams K, Selaya G, Armenteras D, Bilbao BA, Xaud HAM, Rivera-Lombardi R, Ferreira J, Aragão LEOC, Jones CD, Wiltshire AJ. 2022. An alert system for Seasonal Fire probability forecast for South American Protected Areas. Clim Resil Sustain 1:e19. https://doi.org/10.1002/cli2.19.

Aragão LEOC, Malhi Y, Roman-Cuesta RM, Saatchi S, Anderson LO, Shimabukuro YE. 2007. Spatial patterns and fire response of recent Amazonian droughts. Geophys Res Lett 34:L07701.

Archibald S, Bond WJ, Hoffmann W, Lehmann C, Staver C, Stevens N. 2019. Distribution and Determinants of Savannas. In: Scogings PF, Sankaran M, Eds. Savanna Woody Plants and Large Herbivores, 1st edn. Hoboken: Wiley. pp 1–24. https://doi.org/10.1002/9781119081111.ch1.

Armenteras D, Romero M, Galindo G. 2005. Vegetation fire in the savannas of the Llanos Orientales of Colombia. World Resour Rev 17:531–543.

Armenteras D, González TM, Vargas JO, Meza Elizalde MC, Oliveras I. 2020. Incendios en ecosistemas del norte de Suramérica: avances en la ecología del fuego tropical en Colombia, Ecuador y Perú. Caldasia 42:1–16.

Armenteras D, Meza MC, González TM, Oliveras I, Balch JK, Retana J. 2021. Fire threatens the diversity and structure of tropical gallery forests. Ecosphere 12:e03347. https://doi.org/10.1002/ecs2.3347.

Barreto JS, Armenteras D. 2020. Open data and machine learning to model the occurrence of fire in the ecoregion of ''Llanos Colombo–Venezolanos.'' Remote Sens 12:3921.

Beer C, Reichstein M, Tomelleri E, Ciais P, Jung M, Carvalhais N, Rödenbeck C, Arain MA, Baldocchi D, Bonan GB, Bondeau A, Cescatti A, Lasslop G, Lindroth A, Lomas M, Luyssaert S, Margolis H, Oleson KW, Roupsard O, Veenendaal E, Viovy N, Williams C, Woodward FI, Papale D. 2010. Terrestrial gross carbon dioxide uptake: global distribution and covariation with climate. Science 329:834–838.

Bernardino PN, Dantas VL, Hirota M, Pausas JG, Oliveira RS. 2022. Savanna–Forest coexistence across a fire gradient. Ecosystems 25:279–290.

Berrio J-C, Wouters H, Hooghiemstra H, Carr AS, Boom A. 2012. Using Paleoecological Data to Define Main Vegetation Dynamics Along the Savanna–Forest Ecotone in Colombia: Implications for Accurate Assessment of Human Impacts. In: Myster RW, Ed. Ecotones Between Forest and Grassland, . New York: Springer. pp 209–225. https://doi.org/10.1007/978-1-4614-3797-0_9.

Bombardi RJ, Kinter JL, Frauenfeld OW. 2019. A global gridded dataset of the characteristics of the rainy and dry seasons. Bull Am Meteorol Soc 100:1315–1328.

Borghetti F, Barbosa E, Ribeiro L, Ribeiro JF, Walter BMT. 2019. South American Savannas. In: Scogings PF, Sankaran M, Eds. Savanna Woody Plants and Large Herbivores, 1st edn. Hoboken: Wiley. pp 77–122. https://doi.org/10.1002/9781119081111.ch4.

Calders K, Armston J, Newnham G, Herold M, Goodwin N. 2014. Implications of sensor configuration and topography on vertical plant profiles derived from terrestrial LiDAR. Agric For Meteorol 194:104–117.

Case MF, Staver AC. 2018. Soil texture mediates tree responses to rainfall intensity in African savannas. New Phytol 219:1363–1372.

Chuvieco E, Lizundia-Loiola J, Pettinari ML, Ramo R, Padilla M, Tansey K, Mouillot F, Laurent P, Storm T, Heil A, Plummer S. 2018. Generation and analysis of a new global burned area product based on MODIS 250 m reflectance bands and thermal anomalies. Earth Syst Sci Data 10:2015–2031.

Ciemer C, Boers N, Hirota M, Kurths J, Müller-Hansen F, Oliveira RS, Winkelmann R. 2019. Higher resilience to climatic disturbances in tropical vegetation exposed to more variable rainfall. Nat Geosci 12:174–179.

D'Onofrio D, Sweeney L, von Hardenberg J, Baudena M. 2019. Grass and tree cover responses to intra-seasonal rainfall variability vary along a rainfall gradient in African tropical grassy biomes. Sci Rep 9:2334.

Dantas VL, Pausas JG. 2022. The legacy of the extinct Neotropical megafauna on plants and biomes. Nat Commun 13:129.

Daskin JH, Aires F, Staver AC. 2019. Determinants of tree cover in tropical floodplains. Proc R Soc B Biol Sci 286:20191755.

DiMiceli, C, Carroll, M, Sohlberg, R, Kim, D, Kelly, M, Townshend, J. 2015. MOD44B MODIS/Terra Vegetation Continuous Fields Yearly L3 Global 250m SIN Grid V006. NASA EOSDIS Land Processes DAAC. Accessed 2020-12-22 from https://doi.org/10.5067/MODIS/MOD44B.006.

Dubayah R, Blair JB, Goetz S, Fatoyinbo L, Hansen M, Healey S, Hofton M, Hurtt G, Kellner J, Luthcke S, Armston J, Tang H, Duncanson L, Hancock S, Jantz P, Marselis S, Patterson PL, Qi W, Silva C. 2020. The global ecosystem dynamics investigation: High-resolution laser ranging of the Earth's forests and topography. Sci Remote Sens 1:100002.

ESA. 2017. Land cover CCI Product User Guide Version 2.0, available at: http://maps.elie.ucl.ac.be/CCI/viewer/download/.

Fan Y, Li H, Miguez-Macho G. 2013. Global patterns of groundwater table depth. Science 339:940–943.

Fick SE, Hijmans RJ. 2017. WorldClim 2: new 1 km spatial resolution climate surfaces for global land areas. Int J Climatol 37:4302–4315.

Funk C, Peterson P, Landsfeld M, Pedreros D, Verdin J, Shukla S, Husak G, Rowland J, Harrison L, Hoell A, Michaelsen J. 2015. The climate hazards infrared precipitation with stations—a new environmental record for monitoring extremes. Sci Data 2:150066.

Good SP, Caylor KK. 2011. Climatological determinants of woody cover in Africa. Proc Natl Acad Sci 108:4902–4907.

Gosling WD, Miller CS, Shanahan TM, Holden PB, Overpeck JT, van Langevelde F. 2022. A stronger role for long-term moisture change than for CO_2 in determining tropical woody vegetation change. Science 376:653–656.

Hengl T, Mendes de Jesus J, Heuvelink GBM, Ruiperez Gonzalez M, Kilibarda M, Blagotić A, Shangguan W, Wright MN, Geng X, Bauer-Marschallinger B, Guevara MA, Vargas R, MacMillan RA, Batjes NH, Leenaars JGB, Ribeiro E, Wheeler I, Mantel S, Kempen B. 2017. SoilGrids250m: Global gridded soil information based on machine learning. PLoS ONE 12:e0169748.

Hijmans, RJ. 2020. Geographic data analysis and modeling [R package raster version 3.4–5].

Hirota M, Holmgren M, Van Nes EH, Scheffer M. 2011. Global resilience of tropical forest and savanna to critical transitions. Science 334:232–235.

Hoffmann WA, Geiger EL, Gotsch SG, Rossatto DR, Silva LCR, Lau OL, Haridasan M, Franco AC. 2012. Ecological thresholds at the savanna–forest boundary: How plant traits, resources and fire govern the distribution of tropical biomes. Ecol Lett 15:759–768.

Holdo RM, Nippert JB. 2023. Linking resource- and disturbance-based models to explain tree–grass coexistence in savannas. New Phytol 237:1966–1979.

Hoyos N, Correa-Metrio A, Jaramillo C, Villegas JC, Escobar J. 2022. Effects of consecutive dry and wet days on the forest–savanna boundary in north-west South America. Glob Ecol Biogeogr 31:347–361.

IPCC, 2021: Climate Change 2021: The Physical Science Basis. Contribution of Working Group I to the Sixth Assessment Report of the Intergovernmental Panel on Climate Change [Masson-Delmotte, V., P. Zhai, A. Pirani, S.L. Connors, C. Péan, S. Berger, N. Caud, Y. Chen, L. Goldfarb, M.I. Gomis, M. Huang, K. Leitzell, E. Lonnoy, J.B.R. Matthews, T.K. Maycock, T. Waterfield, O. Yelekçi, R. Yu, and B. Zhou (eds.)]. Cambridge University Press. In Press

Jaramillo C. 2023. The evolution of extant South American tropical biomes. New Phytol.

Jarvis, A, Reuter, HI, Nelson, A, & Guevara, E. 2008. Hole-filled SRTM for the globe Version 4. available from the CGIAR-CSI SRTM 90m Database (http://srtm.csi.cgiar.org), 15, 25–54.

Langan L, Higgins SI, Scheiter S. 2017. Climate-biomes, pedo-biomes or pyro-biomes: which world view explains the tropical forest–savanna boundary in South America? J Biogeogr 44:2319–2330.

Lehmann CER, Archibald SA, Hoffmann WA, Bond WJ. 2011. Deciphering the distribution of the savanna biome. New Phytol 191:197–209.

Lehmann CER, Anderson TM, Sankaran M, Higgins SI, Archibald S, Hoffmann WA, Hanan NP, Williams RJ, Fensham RJ, Felfili J, Hutley LB, Ratnam J, San Jose J, Montes R, Franklin D, Russell-Smith J, Ryan CM, Durigan G, Hiernaux P, Haidar R, Bowman DMJS, Bond WJ. 2014. Savanna vegetation–fire–climate relationships differ among continents. Science 343:548–552.

Li Y, Brando PM, Morton DC, Lawrence DM, Yang H, Randerson JT. 2022. Deforestation-induced climate change reduces carbon storage in remaining tropical forests. Nat Commun 13:1964.

Lizundia-Loiola J, Pettinari ML, Chuvieco E. 2020. Temporal anomalies in burned area trends: satellite estimations of the Amazonian 2019 fire crisis. Remote Sens 12:151.

Lloyd J, Domingues TF, Schrodt F, Ishida FY, Feldpausch TR, Saiz G, Quesada CA, Schwarz M, Torello-Raventos M, Gilpin M, Marimon BS, Marimon-Junior BH, Ratter JA, Grace J, Nardoto GB, Veenendaal E, Arroyo L, Villarroel D, Killeen TJ, Steininger M, Phillips OL. 2015. Edaphic, structural and physiological contrasts across Amazon Basin forest–savanna ecotones suggest a role for potassium as a key modulator of tropical woody vegetation structure and function. Biogeosciences 12:6529–6571.

Lloyd J, Goulden ML, Ometto JP, Patiño S, Fyllas NM, Quesada CA. 2009. Ecophysiology of forest and savanna vegetation. In: Keller M, Bustamante M, Gash J, Silva Dias P, editors. Geophysical Monograph Series. Vol. 186. Washington, D. C.: American Geophysical Union. pp 463–84. https://doi.org/10.1029/2008GM000740.

Malhi Y, Aragão LEOC, Galbraith D, Huntingford C, Fisher R, Zelazowski P, Sitch S, McSweeney C, Meir P. 2009. Exploring the likelihood and mechanism of a climate-change-induced dieback of the Amazon rainforest. Proc Natl Acad Sci 106:20610–20615.

Marselis SM, Tang H, Armston J, Abernethy K, Alonso A, Barbier N, Bissiengou P, Jeffery K, Kenfack D, Labrière N, Lee S-K, Lewis SL, Memiaghe H, Poulsen JR, White L, Dubayah R. 2019. Exploring the relation between remotely sensed vertical canopy structure and tree species diversity in Gabon. Environ Res Lett 14:094013.

McCullagh P, Nelder JA. 1983. Generalized Linear Models, 2nd edn. Milton Park: Routledge. https://doi.org/10.1201/9780203753736.

Meeussen C, Govaert S, Vanneste T, Calders K, Bollmann K, Brunet J, Cousins SAO, Diekmann M, Graae BJ, Hedwall P-O, Krishna Moorthy SM, Iacopetti G, Lenoir J, Lindmo S, Orczewska A, Ponette Q, Plue J, Selvi F, Spicher F, Tolosano M, Verbeeck H, Verheyen K, Vangansbeke P, De Frenne P. 2020. Structural variation of forest edges across Europe. For Ecol Manag 462:117929.

Meza MC, Espelta JM, González TM, Armenteras D. 2023. Fire reduces taxonomic and functional diversity in Neotropical moist seasonally flooded forests. Perspect Ecol Conserv. S2530064423000275.

Newberry BM, Power CR, Abreu RCR, Durigan G, Rossatto DR, Hoffmann WA. 2020. Flammability thresholds or flammability gradients? Determinants of fire across savanna–forest transitions. New Phytol 228:910–921.

Oliveras I, Malhi Y. 2016. Many shades of green: the dynamic tropical forest–savannah transition zones. Philos Trans R Soc B Biol Sci 371:20150308.

Paredes-Trejo FJ, Barbosa HA, Lakshmi Kumar TV. 2017. Validating CHIRPS-based satellite precipitation estimates in Northeast Brazil. J Arid Environ 139:26–40.

Pellegrini AFA. 2016. Nutrient limitation in tropical savannas across multiple scales and mechanisms. Ecology 97:313–324.

R Core Team 2022. R: A language and environment for statistical computing. R Foundation 858 for Statistical Computing, Vienna, Austria. URL https://www.R-project.org/.

Ritter F, Berkelhammer M, Garcia-Eidell C. 2020. Distinct response of gross primary productivity in five terrestrial biomes to precipitation variability. Commun Earth Environ 1:34.

Rodríguez-Iturbe I, Porporato A. 2005. Ecohydrology of Water-Controlled Ecosystems: Soil Moisture and Plant Dynamics. 1st ed. Cambridge University Press https://www.cambridge.org/core/product/identifier/9780511535727/type/book. Last accessed 27/05/2022.

Romero-Ruiz M, Etter A, Sarmiento A, Tansey K. 2010. Spatial and temporal variability of fires in relation to ecosystems, land tenure and rainfall in savannas of northern South America: Spatial and temporal variability of fires. Glob Change Biol 16:2013–2023.

Sato H, Kelley DI, Mayor SJ, Martin Calvo M, Cowling SA, Prentice IC. 2021. Dry corridors opened by fire and low CO_2 in Amazonian rainforest during the last glacial maximum. Nat Geosci 14:578–585.

Schwartz NB, Lintner BR, Feng X, Powers JS. 2020. Beyond MAP: A guide to dimensions of rainfall variability for tropical ecology. Biotropica 52:1319–1332.

Staal A, Fetzer I, Wang-Erlandsson L, Bosmans JHC, Dekker SC, van Nes EH, Rockström J, Tuinenburg OA. 2020. Hysteresis of tropical forests in the 21st century. Nat Commun 11:4978.

Stark SC, Breshears DD, Aragón S, Villegas JC, Law DJ, Smith MN, Minor DM, Assis RL, Almeida DRA, Oliveira G, Saleska SR, Swann ALS, Moura JMS, Camargo JL, Silva R, Aragão LEOC, Oliveira RC. 2020. Reframing tropical savannization: Linking changes in canopy structure to energy balance alterations that impact climate. Ecosphere 11:e03231. https://doi.org/10.1002/ecs2.3231.

Staver AC, Archibald S, Levin SA. 2011. The global extent and determinants of savanna and forest as alternative biome states. Science 334:230–232.

Valencia S, Marín DE, Gómez D, Hoyos N, Salazar JF, Villegas JC. 2023. Spatio-temporal assessment of Gridded precipitation products across topographic and climatic gradients of Colombia. Atmos Res 285:106643.

Veenendaal EM, Torello-Raventos M, Miranda HS, Sato NM, Oliveras I, van Langevelde F, Asner GP, Lloyd J. 2018. On the relationship between fire regime and vegetation structure in the tropics. New Phytol 218:153–166.

Xu X, Medvigy D, Trugman AT, Guan K, Good SP, Rodriguez-Iturbe I, Sykes M. 2018. Tree cover shows strong sensitivity to precipitation variability across the global tropics. Glob Ecol Biogeogr 27:450–460.

Yan K, Park T, Yan G, Liu Z, Yang B, Chen C, Nemani R, Knyazikhin Y, Myneni R. 2016. Evaluation of MODIS LAI/FPAR Product Collection 6. Part 2: Validation and Intercomparison. Remote Sens 8:460.

Zeng Z, Chen A, Piao S, Rabin S, Shen Z. 2014. Environmental determinants of tropical forest and savanna distribution: A quantitative model evaluation and its implication: Tropical forest and savanna distribution. J Geophys Res Biogeosci 119:1432–1445.

Zomer RJ, Trabucco A, Bossio DA, Verchot LV. 2008. Climate change mitigation: A spatial analysis of global land suitability for clean development mechanism afforestation and reforestation. Agric Ecosyst Environ 126:67–80.